MODULAR INTERCHANGEABLE HIGH POWER HELICAL ANTENNAS

M.B. Lara, M.G. Mayes, W.C. Nunnally, T.A. Holt and J.R. Mayes
Applied Physical Electronics L C , PO Box 341149
Austin, TX, USA

Abstract

Helical antennas are very appealing for their conformal and relatively small geometries. Moreover, helical antennas can be impulse excited, producing several cycles of resonant energy at a designed frequency, or resonantly-driven by a frequency matched resonator. Applied Physical Electronics, L.C. has previously reported results from impulse excited helical antennas. Those efforts have been continued to result in a family of interchangeable antennas sourced by a common compact pulse power source. This paper describes the system, including the pulse power and the helical antenna loads, supported by simulations and experimental results.

I. BACKGROUND

In 1946, J.D. Krauss discovered that a coaxial-fed helix of 1λ circumference produced a circularly polarized beam which increased in directivity with each additional turn [1]. Since then, the helical antenna has been used prolifically in both communication and directed-energy applications.

Work performed in [2] demonstrated that a helical antenna shock-excited by a Marx generator would radiate a wideband signal at a center frequency defined by the circumference of the helix. Further research revealed that the radiated field-strength of a Marx generator-driven helical-antenna was limited by the following [3]&[4]:

1.) Breakdown at the antenna-feed interface

2.) High VSWR resulting from the high-impedance transition from a coaxial geometry to the antenna

3.) Un-optimized ground plane and reflector geometries

By focusing on solutions to the aforementioned limitations, a design was developed capable of radiating high-power wideband pulses in a relatively compact form factor. Furthermore, frequency-agility was provided through the design of a modular/interchangeable antenna feed, allowing multiple antennas to be connected to a common source.

II. INTERCHANGEABLE ANTENNA DESIGN

Figure 1 shows a comparison of the 1-GHz, 750-MHz, and 400-MHz helical antennas. Each of the modules include a helical antenna, quarter-wave transformer, ground-plane, conical reflector and a coaxial cable-connection/transition capable of being attached to a section of Dielectric Sciences™ 2158, 41-Ohm coaxial cable. The MG15-3C-940PF Marx generator detailed in the following section is also designed to mate to this same cable [5]. This feature facilitated an interchangeable feed system between the three antenna modules and a single generator. A summary of the design parameters for each antenna module is listed below in Table 1.

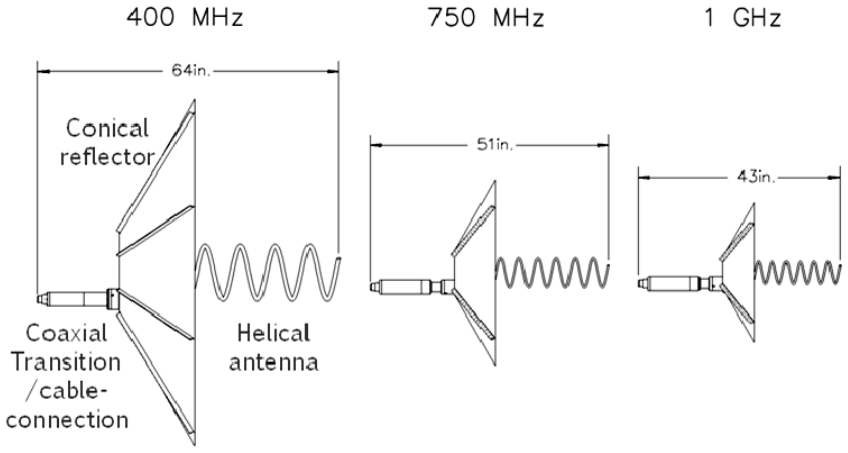

Figure 1. Modular interchangeable high-power helcial antennas

Ξ email: mlara@apelc.com

Table 1. Helical antenna design parameters

Antenna	Turn-turn	Diameter	Ground Dia	# Turns
400-MHz	λ/4	(1.2 λ)/π	.75∗λ	6
750-MHz	λ/4	(1.2 λ)/π	.75∗λ	8
1-GHz	λ/4	(1.2 λ)/π	.75∗λ	8

III. MARX GENERATOR SOURCES

Two separate Marx generators were utilized for this effort: The first, a 15 stage, 600 kV erected-voltage generator (MG15-3C-940PF) [5], was used to directly impulse-excite a 400 MHz helical antenna. The second, a 17 stage, 680 kV erected-voltage Marx generator (MG17-1C-500PF) was used in conjunction with a pulse-conditioning section to resonantly source a 1 GHz helical antenna. The specifications for the two generators are listed in Table 2 and Table 3

Table 2. Specifications of the MG15-3C-940PF

Parameter	Value	Units
Length	82	cm
Diameter	16.5	cm
Weight	16	kg
Number of Stages	15	--
Erected Voltage (open circuit)	600	kV
Charge Voltage	40	kV
Capacitance per Stage	2.8	nF
Erected Capacitance	188	pF
Source Impedance	52	Ohms

To directly impulse-excite the antenna load, it was necessary to generate frequency content which was within the bandwidth of the antenna. The formula given in Eq.1 shows that the sourcing of a 400-MHz antenna requires a risetime of at least 875 ps.

$$f_c = 0.35 * \frac{1}{t_r}. \qquad (1)$$

The un-optimized MG15-3C-940PF generates a double exponential waveform with a risetime on the order of 3-5 ns. To achieve the required sub-nanosecond risetime, a peaking switch was designed and constructed [5]. Figure 2 shows a comparison of the Marx generator output with and without the peaking section. With the peaking section, the generator is capable of a 10-80% risetime of 500 ps at a 30 kV charge (850 ps 10-90% at 20 kV charge).

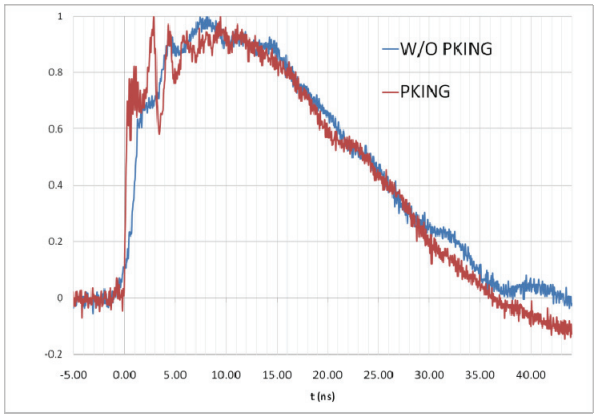

Figure 2. MG15-3C-940PF measured waveform with (red) and without (blue) peaking (30 kV charge voltage)

A. MG17-1C-500PF

The MG17-1C-500PF was chosen as a pulsed power source because of the close match in erected capacitance to the intrinsic capacitance of the attached resonator circuit. Furthermore, the physical dimensions of the generator ensured a simple mechanical connection to the resonator hardware. Figure 10 shows the MG17-1C-500PF with the attached resonator.

Table 3. Specifications of the MG17-1C-500PF

Parameter	Value	Units
Length	1.02	m
Diameter	7.62	cm
Weight	5	kg
Number of Stages	17	--
Erected Voltage (open circuit)	680	kV
Charge Voltage	40	kV
Capacitance per Stage	500	pF
Erected Capacitance	29	pF
Source Impedance	150	Ohms

IV. SHOCK-EXCITED 400-MHZ HELICAL ANTENNA

A. Simulation

CST Microwave Studio™ was used to simulate the 400-MHz helical antenna with a conical reflector. The design of the reflector was sourced directly from [1].

Results of the simulation (Figure 3) show an increase from 12.9 dB gain without the conical reflector, to 15 dB gain with the reflector. This is also accompanied by a significant reduction in back-lobe radiation as would be expected.

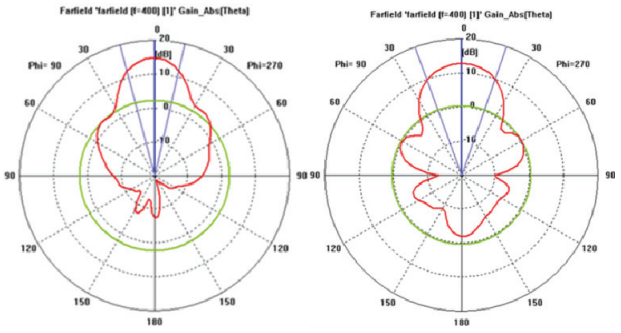

Figure 3. Simulated gain comparison for the 400-MHz helical antenna with (left) and without (right) the conical reflector

B. Vector Network Analyzer (VNA) measurements

The 400-MHz helical antenna was constructed and S-parameters were acquired on a 10-meter range as shown in Figure 4. The transmitting and receiving antennas were both raised 4 meters above the ground-plane to reduce ground-bounce.

Figure 4. 400-MHz helical antenna VNA testing

As can be seen in Figure 6, the gain measured using a VNA was significantly lower than that predicted in simulation (9 dB vs. 15 dB). The Voltage Standing Wave Ration (VSWR) measurement (Figure 5) revealed that one possible reason for this discrepancy exists in a frequency mismatch between one or more components in the antenna module, as well as reflection losses resulting from abrupt transitions in impedance. The VSWR plot shows that the impedance looking into the antenna feed is closely matched to the source at 320 MHz and 450 MHz, while the gain plot (Figure 6) shows that the antenna radiates the most efficiently at ~400-MHz, as would be expected. An improperly tuned quarter-wavelength matching section and multiple impedance discontinuities are thought to be the cause of this behavior.

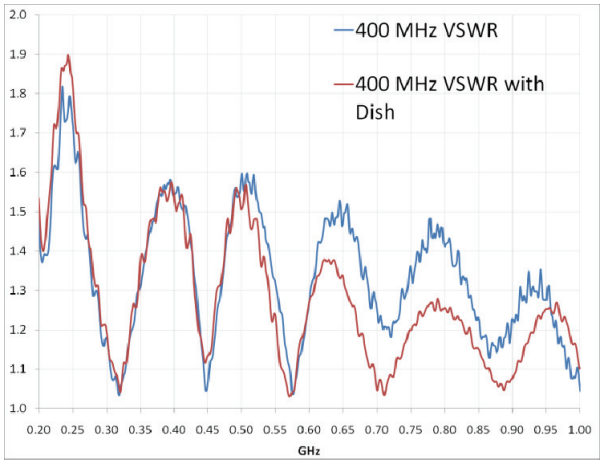

Figure 5. Measured VSWR comparison for the 400-MHz helical antenna with (red) and without (blue) the conical reflector

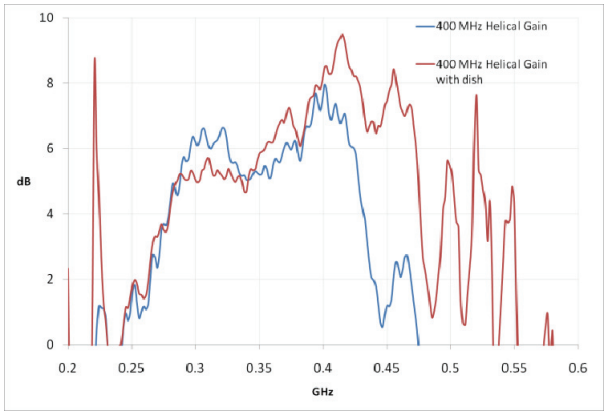

Figure 6. Measured gain comparison for the 400-MHz helical antenna with (red) and without (blue) the conical reflector

C. TDR Measurement

A time domain reflectometer (TDR) was used to verify the impedance associated with each section of the transition from coaxial cable to the antenna. The TDR data, shown Figure 7, begins with a flat line of ~ 1.5 ns in

length representing the 50-Ohm cable running from the TDR to an SMA connector placed at the input to the coaxial transition. An abrupt decrease in impedance is seen after this where the SMA connector comes in close proximity to the housing of the coaxial section. A tapered length of transmission line transitions from 50-Ohms to the 87-Ohm matching section. This section is intended to be a quarter-wave transformer between the cable impedance and the 150-Ohm impedance of the helical antenna. The plot shows the section starting at the intended 87-Ohms and then dipping down to 75-Ohms due to a slight sag in the conductor over the ground plane. From this point forward the impedance increases as the antenna extends outward beyond the ground plane.

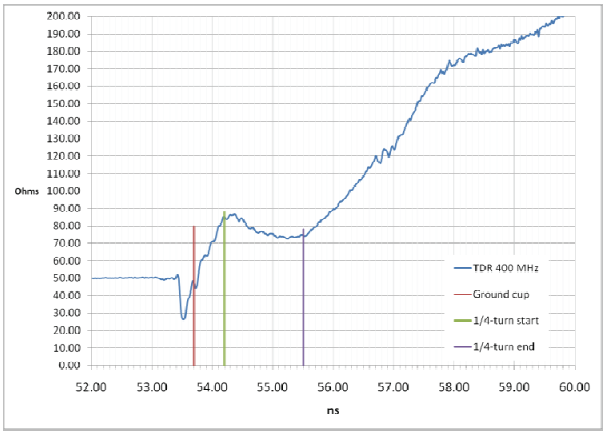

Figure 7. TDR measurement for the 400-MHz helical antenna, transition, and conical reflector

D. High-voltage E-field measurements

Using the peaking-switch-assisted MG15-3C-940PF generator detailed above, the 400-MHz helical antenna and conical reflector produced a field strength of ~100 kV/m as shown in Figure 8.

Using an antenna gain of 15 dB, the radar equation (Eq.2) predicts an electric-field strength of over 300 kV/m for an antenna voltage of 200 kV. The significant reduction in measured field strength is thought to be a result of multiple factors. The first, and most prominent of these is revealed in a comparison of the TDR results to the VSWR measurement. The TDR demonstrates that the quarter-wave matching section is slightly longer than it should be for a center frequency of 400 MHz. Furthermore, the transitions in impedance most likely occur too rapidly, generating substantial voltage reflections. Analysis of the VSWR plot in Figure 5 reveals a good match between 320-MHz and 350-MHz, and a fairly poor match at 400-MHz. This analysis further suggests that the quarter-wavelength section is too long, and that significant voltage reflections are occurring at 400-MHz. Considering this, a lower antenna voltage would be expected, and therefore a lower electric-field strength.

$$E\ (r = 1\ m) = \sqrt{\frac{P_{antenna}}{4\pi\, r^2}\ x\ Gain\ x\ 377}\ \left(\frac{kV}{m}\right) \quad (2)$$

Contradictory to the gain plot of Figure 6, the center frequency of the radiated electric field is 320 MHz. Again, a comparison with the VSWR plot suggests that the quarter-wavelength matching section, and the abrupt impedance transitions, are suppressing the higher frequency content (>350-MHz), causing the helical antenna to radiate well below its designed center frequency. Data taken on the 750-MHz and 1-GHz antennas showed similar behavior (i.e. radiated frequencies well below the designed center frequency).

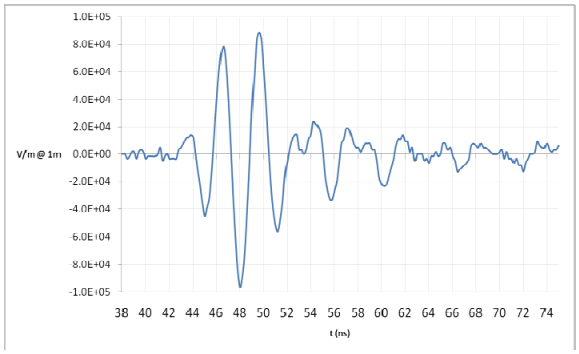

Figure 8. Measured E-field normalized to 1 meter for the 400-MHz helical antenna a conical reflector (30 kV charge voltage)

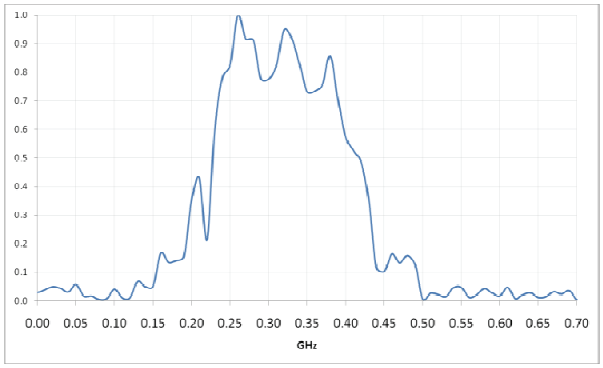

Figure 9. FFT of the measured E-field from the 400-Helical antenna and conical reflector

V. RESONATOR-DRIVEN HELICAL ANTENNA

While impulse-excitation of a helical antenna can result in very high peak-powers on the antenna, the average power is extremely low, considering the low power spectral-density associated with an impulse. Pulse conditioning of the Marx generator output, in theory, remedies this by converting the double-exponential Marx pulse to a damped-sinusoid. This is realized in hardware by pulse-charging a secondary capacitance with the erected output voltage of the generator. A low-side switch closes when the break-down voltage is achieved, and a simple L-C oscillator is formed between the resonator capacitance and the switch inductance.

The integration of a resonator between the MG17-1C-500PF and a helical antenna is demonstrated in Figure 10.

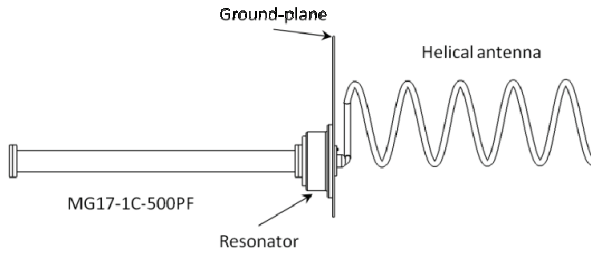

Figure 10. MG17-1C-500PF with attached resonator and helical antenna

Adjustment of the resonator center-frequency was possible through variation in the switch inductance. This provided a means for matching the resonator frequency content to a particular antenna load. The FFT comparison in Figure 12 shows that the spectral content of the resonator voltage closely (but not perfectly) matched the radiated frequency of the antenna.

The helical antenna used for this experiment was designed to have a center frequency of 1-GHz. Additionally, the resonator when tested with a resistive load, exhibited a center frequency of 1-GHz. However, when attached to the antenna, the center frequency of the resonator dropped to 900-MHz (most likely a result of added capacitance) and the radiated field from the helical antenna yielded a center frequency closer to 850-MHz. A parallel to the impulse-excited helical antenna can be made in that the helical antenna, although designed for one particular center frequency, will radiate at a lower frequency when driven below its design frequency. This out-of-band operation also provides one explanation for the low field strength (~10 kV/m) shown in Figure 11.

The second factor affecting the radiated field strength was simply the voltage making it onto the antenna. Figure 13 shows that the resonator capacitance was only charged to 25 kV before the switch closed. For this experiment, the hold-off voltage was limited by the rated pressure of the resonator housing (50 psi/.345 MPa).

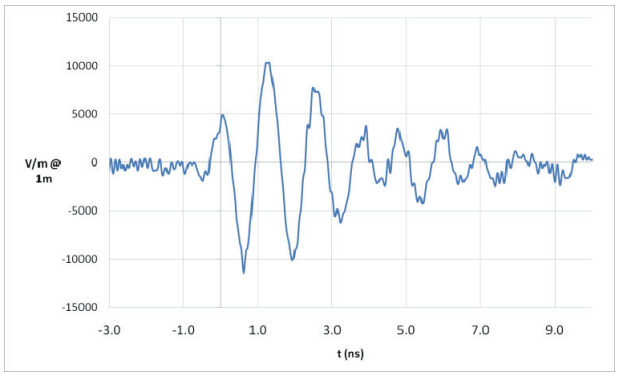

Figure 11. E-field normalized to 1 meter for the resonator-driven helical antenna

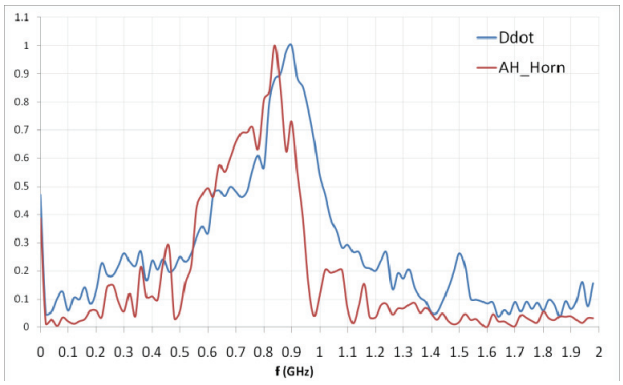

Figure 12. FFT comparison of the radiated E-field (red) and the resonator voltage (blue) for the resonator-driven helical antenna

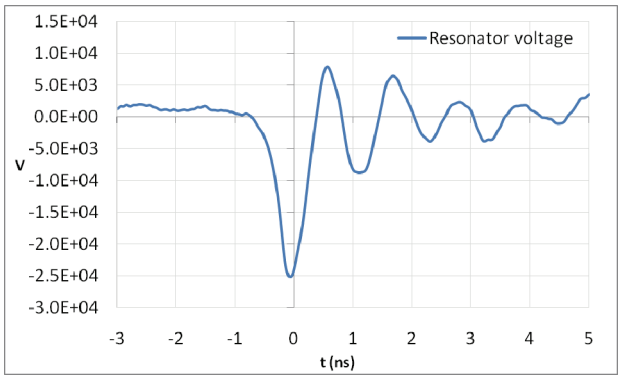

Figure 13. Resonator capacitor voltage

VI. CONCLUSIONS

Two separate antenna configurations were designed, simulated, fabricated and tested. The impulse-excited, interchangeable, helical-antenna-modules demonstrated an interconnect design that could operate multiple antennas with a single pulsed-power source. However, the necessity for a faster rise-time onto the antenna will be needed for all the modules to operate at their designed center frequency. The radiated field-strength of the device was limited by the gain of the antenna and the power on the antenna. Future work in this area would

improve upon the design by more closely tuning the quarter-wave matching section to the antenna, and by making a smoother transition in impedance.

The resonator-driven helical antenna demonstrated that it was possible to generate frequency content near 1 GHz in an integrated package with the Marx generator and helical antenna. The radiated field strength of this device was limited by matching of the resonator center frequency to the antenna center frequency, and by the voltage making it onto the antenna.

VII. REFERENCES

[1] John David Kraus, Antennas, 2nd edition. 1988.

[2] J. R. Mayes, W. J. Carey, W. C. Nunnally, and L. L. Altgilbers, "The Marx Generator as an Ultra Wideband Source," Proc. of the 13th IEEE International Pulsed Power Conference, Las Vegas, pp. 1665 – 1669, 2001.

[3] J. R. Mayes et al., "Helical Antennas for High Powered RF," Proc. of the 17th IEEE International Pulsed Power Conference, Washington D.C, pp. 484 – 488, 2009.

[4] Dr. David Giri, Protech, Berkeley CA.

[5] T.Holt et al., "A Versatile Marx Generator for Use in Directed Energy and Effects Testing Applications", presented at the 18th IEEE International Pulsed Power Conference.